



# Diphenylaminocarbazoles by 1,8-functionalization of carbazole: Materials and application to phosphorescent organic light-emitting diodes



Shahid Ameen<sup>a, b, c</sup>, Seul Bee Lee<sup>a, b</sup>, Sung Cheol Yoon<sup>a, b</sup>, Jaemin Lee<sup>a, b, \*</sup>,  
Changjin Lee<sup>a, b, \*\*</sup>

<sup>a</sup> Advanced Materials Division, Korea Research Institute of Chemical Technology, Daejeon 305-600, Republic of Korea

<sup>b</sup> Nanomaterials Science and Engineering Major, University of Science & Technology (UST), Daejeon 305-333, Republic of Korea

<sup>c</sup> Department of Chemistry, Kohat University of Science and Technology (KUST), Kohat 26000, Pakistan

## ARTICLE INFO

### Article history:

Received 10 July 2015

Received in revised form

26 August 2015

Accepted 28 August 2015

Available online 5 September 2015

### Keywords:

Carbazole

Diphenylamine

Phosphorescence

OLED

Host

Triplet energy

## ABSTRACT

A series of novel carbazole-based materials, **DPACz1**, **DPACz2** and **DPACz3** having diphenylamino moieties at 1- and 8-positions of carbazole have been synthesized and characterized for the first time. The introduction of diphenylamino substituents at 1- or 1,8-positions of carbazole resulted into increase of the band-gap compared with the previously reported 3,6- or 2,7-substituted ones. The HOMO levels increased from **DPACz1** to **DPACz2** with the addition of one additional diphenylamino unit, and further increased in case of **DPACz3**, a dimer of **DPACz1** having a benzidine moiety. The materials have high triplet energy levels of 2.68, 2.60 and 2.45 eV, respectively. Based on suitable HOMO levels and high triplet energies, the newly synthesized diphenylaminocarbazoles were investigated for their potential as solution-processable host materials for green phosphorescent OLEDs with the device configuration, [ITO/PEDOT:PSS/Emitting layer/TPBi/CsF/Al]. All the devices emitted typical green light with high luminance and had low turn-on voltages along with good luminous efficiencies which were further improved by adjusting charge balance using PBD, as a co-host. The basic characteristics and the preliminary OLED results showed the usefulness of our new materials, and this kind of 1-/1,8-substitution of carbazole would open a new way of materials design.

© 2015 Elsevier Ltd. All rights reserved.

## 1. Introduction

Organic electronic devices *viz.* organic light-emitting diodes (OLEDs), organic photovoltaics (OPVs) and organic field effect transistors (OFETs) have gained tremendous attention in both academia and industry due to their vast applications in the future electronics technologies [1,2]. OLEDs are in commercial applications like smart phones and TV displays, ranging from a few inches to a few scores of inches. In contrast to the state-of-the art vacuum deposition method, fabrication of OLEDs using the solution process

methods such as spin-coating or inkjet printing makes the fabrication process easy as well as economical in terms of fabrication cost and wastage of the materials. Another major advantage of the solution process is the fabrication of large area devices that is troublesome by the vacuum deposition. Based upon the ease and cost-effectiveness of the solution-process method, a large amount of data about solution processed OLEDs is available [3].

Phosphorescent organic light-emitting diodes (PHOLEDs) have attracted much interest because of their potential to harvest 100% internal quantum efficiencies due to involvement of the both singlet and triplet excitons and hence increasing the external quantum efficiencies of the devices [4]. In this case, the phosphorescent emitter, generally a heavy metal organometallic complex, is dispersed in a host material. A good host material should have both of the two characteristics, i.e. a) a higher triplet energy than that of the guest emitter for efficient energy transfer from host to guest and suppression of back transfer from dopant to the host, b) appropriately spaced HOMO and LUMO energy levels for a balanced

\* Corresponding author. Advanced Materials Division, Korea Research Institute of Chemical Technology, 141 Gajeong-ro, Yuseong-gu, Daejeon 305-600, Republic of Korea. Tel.: +82 42 860 7212; fax: +82 42 860 7200.

\*\* Corresponding author. Advanced Materials Division, Korea Research Institute of Chemical Technology, 141 Gajeong-ro, Yuseong-gu, Daejeon 305-600, Republic of Korea. Tel.: +82 42 860 7208; fax: +82 42 860 7200.

E-mail addresses: [jminlee@kriict.re.kr](mailto:jminlee@kriict.re.kr) (J. Lee), [cjlee@kriict.re.kr](mailto:cjlee@kriict.re.kr) (C. Lee).

transport of the holes and electrons injected from the respective electrodes.

Carbazole-based materials have gained special attention for their use as hole-transport materials [5–8], luminescent agents [9–11], and host materials for phosphorescent OLEDs [12–17] because of their high triplet energies,  $E_T$  (up to 3.05 eV), excellent hole-transporting properties, and suitable HOMO levels. Likewise, triaryl amines have high triplet energy and good hole transport properties, so, these materials are amongst the best studied classes of materials for OLED applications [18–20].

A number of carbazole-derivatives having substitution at 2-, 7-, 3-, 6- and 9-positions, have been synthesized and tested for their role as host or hole transport materials for OLEDs [21–24]. However, carbazoles with substituents at 1- and 8-positions have been relatively rarely reported [25–30], particularly for their use in OLEDs [31,32]. Substitutions at 1- and 8-positions of carbazole occur once the more active positions i.e. 3, 6 and 9, are first occupied [33]. Carbazole-based triaryl amines such as those obtained by appending diphenylamino units at 3-, 6- [34–37] and 2-, 7-positions [38,39] have been reported previously for their hole transport properties, but to the best of our knowledge, no report is there for carbazoles with diphenylamino-units appended at only 1- and 8-positions and the use of such materials for OLED applications. Regarding the importance of substituents at 1- and 8-positions of carbazole with respect to the host materials, it has been found that substitution at 1- and 8-positions results into materials with higher triplet energy levels than those with substitution at 2-,7- or 3-,6-positions [31]. It is intriguing, therefore, to further elaborate the substituent effect at 1- and 8-positions of carbazole system using functionalities having good charge transport properties such as diphenylamino for their use as host as well as hole transport materials in OLEDs.

Here, we report the design and synthesis of a series of three carbazole derivatives having diphenylamine units at 1- and 8-positions followed by fabrication and studies of green phosphorescent OLED devices using these materials as hosts. The materials were designed in such a way that we started with a carbazole system with one diphenylamine unit at 1-position only, **DPACz1**, followed by two diphenylamines at 1- and 8-positions, **DPACz2**. In order to investigate the effect of increasing the conjugation length of the **DPACz1** system, we also synthesized a TPD [N,N'-bis(3-methylphenyl)-N,N'-bis(phenyl)-benzidine] analogue, **DPACz3**,

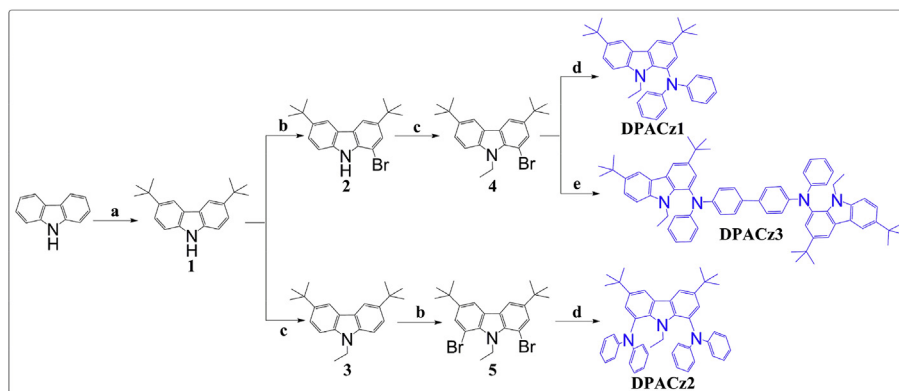
which may be considered as a dimer of **DPACz1** through para-positon of one of the phenyl rings of the diphenylamino moiety.

## 2. Results and discussion

### 2.1. Syntheses of materials

Synthesis of the carbazole derivatives presented in this article is depicted in Scheme 1. The three host materials were prepared starting from commercial carbazole. Intermediate (1) was synthesized as previously reported [40]. The monobromo intermediate (4) was prepared by first bromination of (1) with NBS to get (2) [41] followed by N-alkylation with bromoethane in the presence of NaOH in acetone [42]. It is important to mention here that this pathway for the preparation of (4) was found to be much easier as compared to the previously reported method [31] of doing N-alkylation first and then bromination which resulted into the formation of both mono- and dibromocarbazoles, (4) and (5) respectively, which were not easily separable by column chromatography (due to very close  $R_f$  values) or by recrystallization (due to quite similar solubilities). In our method although the bromination of (1) using 1:1 molar ratio of the reactant and NBS resulted into the appearance of the 1,8-dibromocarbazole as a very small impurity but the  $R_f$  values of the two bromocarbazoles with free 'NH' group were much different to allow easy purification of (4) by column chromatography. The dibromo intermediate (5) was prepared following a reported method [33]. The mono- and dibrominated intermediates (4) and (5) were converted to the final products (**DPACz1**) and (**DPACz2**), respectively, by Buchwald–Hartwig cross-coupling reaction with diphenylamine in toluene, using  $\text{Pd}_2(\text{dba})_3$  as catalyst and DPPF or  $t\text{Bu}_3\text{P}$  as co-catalyst, in good yields [38]. For the synthesis of (**DPACz3**), the monobrominated carbazole (4) was cross-coupled with 4,4'-diphenylbenzidine under the above mentioned Buchwald–Hartwig reaction conditions.

All the compounds were purified by column chromatography and/or recrystallization from appropriate solvents and were obtained as white solids. The chemical structures of the final compounds were confirmed by  $^1\text{H}$  NMR (Figs. S1–S3),  $^{13}\text{C}$  NMR (Figs. S4–S6) and high resolution mass spectrometry. All the three final compounds were highly soluble in common organic solvents, such as toluene, chlorobenzene, chloroform, dichloromethane, acetone, tetrahydrofuran etc.



**Reagents and Conditions:** a.  $t\text{BuCl}$ ,  $\text{ZnCl}_2$ , nitromethane, rt b. NBS, DMF, rt c. EtBr, NaOH, TBAB, acetone, reflux d. Diphenylamine,  $\text{Pd}_2(\text{dba})_3$ ,  $t\text{Bu}_3\text{P}$ ,  $t\text{BuONa}$ , toluene,  $\text{N}_2$ , reflux e. Diphenylbenzidine,  $\text{Pd}_2(\text{dba})_3$ ,  $t\text{Bu}_3\text{P}$ ,  $t\text{BuONa}$ , toluene,  $\text{N}_2$ , reflux.

Scheme 1. Syntheses of **DPACz1**, **DPACz2** and **DPACz3**.

## 2.2. Physical properties

Absorption and photoluminescence spectra of the three carbazole derivatives in dichloromethane (DCM) solution, and as spin coated films, at room temperature are shown in Fig. 1a and b,

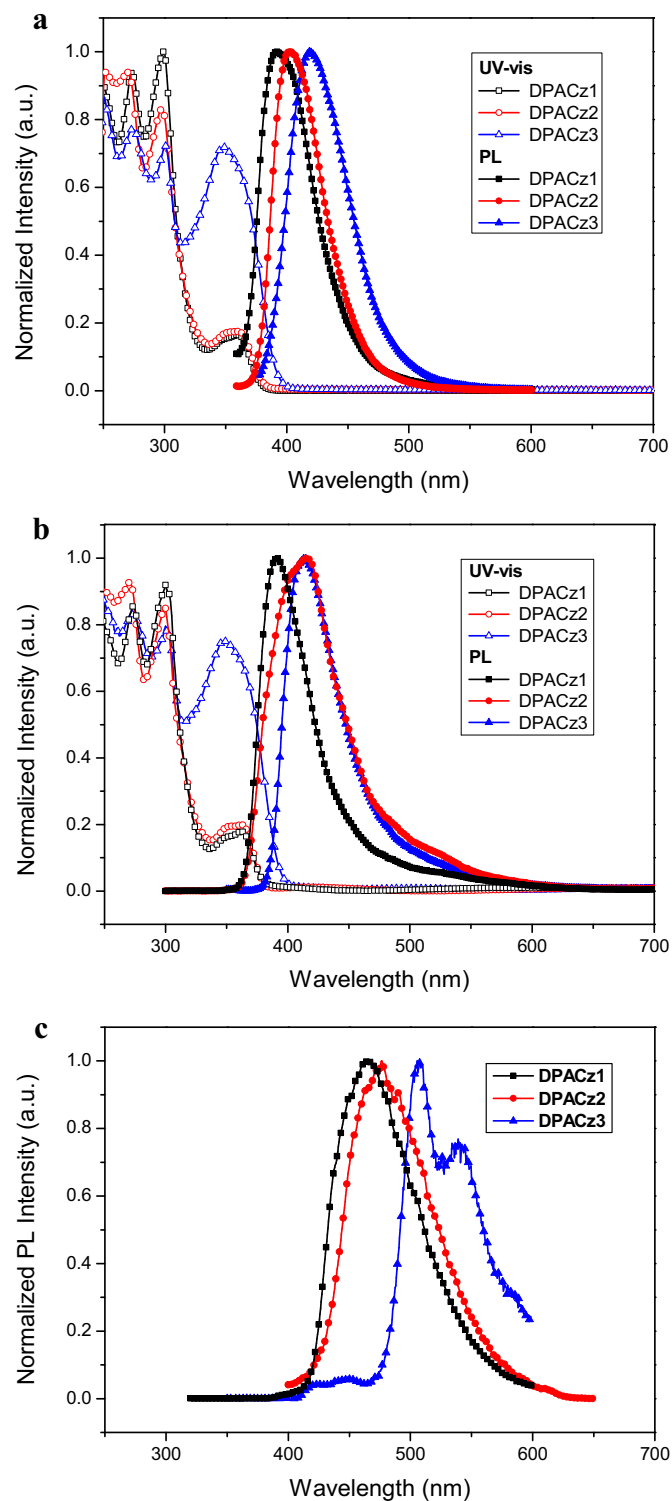


**Fig. 1.** (a) UV–vis and PL spectra of dil. solutions of **DPACz1**, **DPACz2** and **DPACz3** in DCM, (b) UV–vis and PL spectra **DPACz1**, **DPACz2** and **DPACz3** thin films on quartz substrates, (c) Phosphorescent spectra of **DPACz1**, **DPACz2** and **DPACz3** at 77 K.

respectively; and the photophysical data including the wavelengths of the lowest absorption maxima along with the PL emission maxima is presented in Table 1. Both the solution and thin film spectra are nearly identical. The absorption pattern of the three compounds is mutually similar as shown by the spectra, having similarity with the 1,8-fluorenyl substituted carbazoles [31]; particularly, the absorption spectra of **DPACz1** and **DPACz2** are similar showing there is no particular change in the absorption with the increase in the no. of diphenylamine unit at positions 1 and 8 of carbazole. The absorption spectral pattern of **DPACz3**, although similar to the other two compounds, is however, having a prominent increase in the absorption coefficient of the lowest energy band which is due to increased conjugation length through the benzidine system present in this molecule (analogous to TPD) [43–45]. Compared to the 3-, 6- substituted carbazoles, though the  $\lambda_{\text{max}}$  of the lowest energy band is almost not affected by changing the position of diphenylamino functionality from 3-position of carbazole to 1-position but the absorption edge is blue shifted increasing the band gap from 3.04 [30] to 3.28 eV (3.25 as thin film) in case of **DPACz1**. The *tert*-butyl groups may also have played a role due to its bulkiness thereby decreasing the  $\pi$ – $\pi$  interactions between the carbazole systems (investigation on the effect of *tert*-butyl group on the band gap properties of carbazole systems is in progress). The emission spectra of the target compounds in thin film are narrower as compared to those in dilute solution, specially in the shorter wavelength regions of the PL spectra. This effect may be attributed to the bulky *tert*-butyl groups which inhibit  $\pi$ – $\pi$  interactions between the adjacent small molecules. But in case of the thin film PL spectrum of **DPACz2**, an insignificant shouldering occurs towards the longer wavelength region. As it is required for an efficient PhOLED that the triplet energy of the host material should be significantly higher than that of the emitter guest, so that the triplet excitons from the host could easily transfer down the energy gradient to the emitter molecules to be radiatively de-excited to the ground states. Triplet energy levels of the host materials were determined from the highest energy emission peaks of the phosphorescent spectra of their solutions in methyltetrahydrofuran at 77 K (Fig. 1c). The triplet energy levels of the three host materials are also summarized in Table 1. As shown in the table, the triplet energy levels of the three host materials are in range of 2.45–2.68, higher than that of the common green phosphorescent emitter, Ir(mppy)<sub>3</sub> i.e. 2.4 eV, so, these materials, particularly **DPACz1** and **DPACz2**, are suitable as hosts for green OLEDs.

Thermal properties of the new materials were analyzed by differential thermal calorimetry (DSC). DSC curves for the three host materials are shown in Fig. S7, and data are also summarized in Table 1. The  $T_g$  values of the three materials were estimated from the respective DSC curves of the second heating scans.  $T_g$  values for **DPACz1** and **DPACz2** were found, respectively, to be 65 °C and 92 °C whereas  $T_g$  of **DPACz3** was 165 °C. Here, it is obvious that  $T_g$  values increase with the increasing molecular weights ( $M_r$ : 474, 642 and 947, respectively) of these materials [46], however the  $T_g$  value for

**Table 1**  
Physical data of host materials **DPACz1**, **DPACz2** and **DPACz3**.

Compound	$\lambda_{\text{max, abs}}$ (nm)		$\lambda_{\text{max, em}}$ (nm)		$E_g^a$ (eV)	$E_T^b$ (eV)	$T_g^c$ (°C)
	Soln.	Film	Soln.	Film			
<b>DPACz1</b>	360	362	396	391	3.25	2.68	65
<b>DPACz2</b>	360	362	386	416	3.26	2.60	92
<b>DPACz3</b>	348	348	420	414	3.14	2.45	165

<sup>a</sup> Calculated from the absorption edge of the film UV–vis spectra.

<sup>b</sup> Determined from low temperature PL spectra in frozen 2-methyltetrahydrofuran.

<sup>c</sup> Determined from the second heating scan of DSC.

**DPACz3** is comparatively too high due to higher molecular weight and more expanded structure of **DPACz3**. Although the  $T_g$  value of **DPACz1** is not too high but even then this is comparable to the commercially available common host materials with the similar range of molecular weights such as CBP ( $M_r$ , 484;  $T_g$ , 62 °C) and mCP ( $M_r$ , 408;  $T_g$ , 55 °C) [16].

In addition to the optical and thermal properties of the new materials, the film-forming from spin-coating and the surface morphologies were also investigated by atomic force microscopy (AFM). The topographic images of the spin-coated films of each of the materials are shown in Fig. S8. All of the three materials showed negligible differences in surface roughness and showed smooth enough surfaces. The RMS (root mean square) roughness values of the spin-coated films of **DPACz1**, **DPACz2** and **DPACz3** were 0.254 nm, 0.266 nm and 0.251 nm, respectively. This result implies the applicability of our new materials for solution-processing.

### 2.3. Electrochemical properties

The electrochemical properties of the materials were studied through cyclic voltammetry (CV) of the dilute solutions in methylene chloride using tetrabutylammonium hexafluorophosphate as a supporting electrolyte. CV of TPD (Full name necessary) was also measured to compare and estimate the HOMO energy levels of our new materials. The CV graphs of the target compounds are shown in Fig. 2. All the three compounds showed reversible oxidation behaviour which suggested the electrochemical stability of the compounds while used in an OLED. **DPACz3** showed a typical TPD like behaviour in CV.

The first oxidation potentials of **DPACz1**, **DPACz2** and **DPACz3** were observed at 425, 378 and 279 mV, respectively, versus ferrocene/ferrocene<sup>+</sup> while the first oxidation potentials of TPD was 265 mV. Considering  $-5.4$  eV of HOMO energy level of TPD [47], the translated HOMO energy levels of **DPACz1**, **DPACz2** and **DPACz3** were  $-5.56$ ,  $-5.51$  and  $-5.41$  eV, respectively. The LUMO energy levels were calculated by adding the optical band gaps to the HOMO energy levels. The electrochemical data is presented in Table 2.

From **DPACz1** to **DPACz2**, the HOMO energy level of **DPACz2** was slightly increased due to bis-substitution of diphenylamine substituents. **DPACz3** showed the highest HOMO energy level among the three series of materials, which can be attributed to the increased  $\pi$ -conjugation through benzidine structure. It is also

**Table 2**

Electrochemical data of the host materials **DPACz1**, **DPACz2** and **DPACz3**.

Compound	$E_{ox,1/2}$ (mV)	HOMO (eV)	LUMO <sup>a</sup> (eV)
<b>DPACz1</b>	425	$-5.56$	$-2.31$
<b>DPACz2</b>	378	$-5.51$	$-2.25$
<b>DPACz3</b>	279	$-5.41$	$-2.27$

<sup>a</sup> Calculated by adding up the respective optical band gaps and the HOMO values.

noteworthy that the difference of LUMO energy levels of the three compounds is relatively small, which means that arylamine substitution and benzidine structure of carbazole influence mainly the HOMO energy levels.

### 2.4. Quantum chemical calculations

In order to understand the relationship between the geometrical structures of the host materials and the distribution of electron densities over the molecules and hence the electronic properties, DFT calculations at B3LYP and 6-31G (d) levels were performed. The calculation results are shown in Fig. 3. It is obvious that the HOMO levels of these materials are located mainly on the more electron rich diphenylamino moieties and LUMO are located on the carbazole nucleus. As all the three molecules are completely conjugated structures and are non-polar in nature, so, the HOMO and LUMO levels are not well separated rather these are intermixed that may give rise to intramolecular charge transfer.

### 2.5. Device fabrication and measurement

To investigate the potential of our materials as phosphorescent host materials, we first fabricated simple solution-processed green phosphorescent OLEDs adopting the three host materials, **DPACz1**, **DPACz2**, and **DPACz3**. The device configuration was [ITO/PEDOT:PSS (35 nm)/Emitting layer (40 nm)/TPBi (57 nm)/CsF (1 nm)/Al (80 nm)]. The emitting layer was composed of 93 wt% of each of the host materials and 7 wt% of green emitting dopant, Ir(mppy)<sub>3</sub>. Here PEDOT:PSS, TPBi and LiF served as hole-injecting, electron transporting/hole blocking and electron-injecting layers, respectively. The energy levels diagram for the devices is shown in Fig. 4. The OLED devices containing each of the three host materials, **DPACz1**, **DPACz2**, and **DPACz3**, are denominated as **Device 1**, **Device 2**, and **Device 3**, respectively. In addition to the aforementioned three devices, we also fabricated a reference device (**Device 4**) which contains **26DCzPPy** as a host to estimate the relative level of our device results.

Fig. 5 shows the resultant device characteristics and the values are summarized in Table 3. As is clearly seen from the J–V–L curves (Fig. 5a), the turn-on voltage ( $V_{on}$ , recorded at the luminance of 10 cd m<sup>-2</sup>) significantly decreased from 4.6 (**Device 1**) through 3.7 V (**Device 2**) to 3.1 V (**Device 3**). This tendency can be attributed to the reduction of the hole-injection barrier from the ITO/PEDOT:PSS anode to the emitting layer as HOMO levels of each of the host materials in these devices increase from **DPACz1** to **DPACz3**, respectively. The maximum achieved luminance for these devices increased in the order from **Device 3** (4936 cd m<sup>-2</sup>) through **Device 2** (6632 cd m<sup>-2</sup>) to **Device 1** (8050 cd m<sup>-2</sup>). But even **Device 1** could not show comparable maximum luminance to **Device 4**, that is to say the maximum luminance of **Device 1** was about a half of **Device 4**.

Although the maximum luminance values of our new materials were relatively lower than that of the reference, **26DCzPPy**, we could find out an improvement in the device efficiencies, especially in cases of **DPACz1** and **DPACz2**. Fig. 5b shows the luminous efficiency-luminance curves of the four devices. The maximum

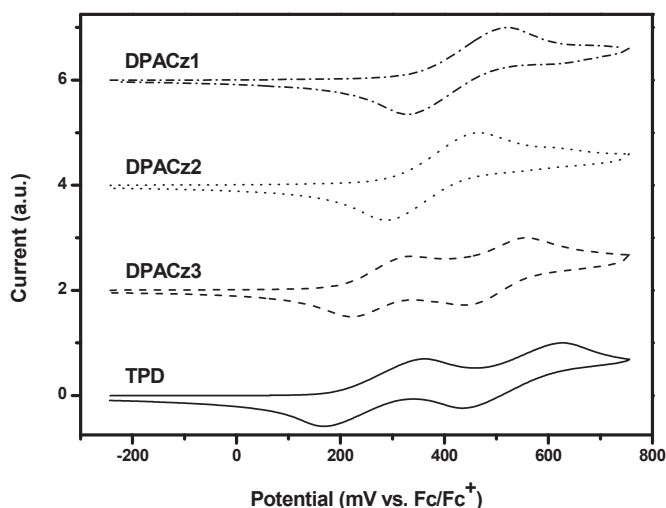


**Fig. 2.** Cyclic voltammograms of TPD and the host materials **DPACz1**, **DPACz2** and **DPACz3**.

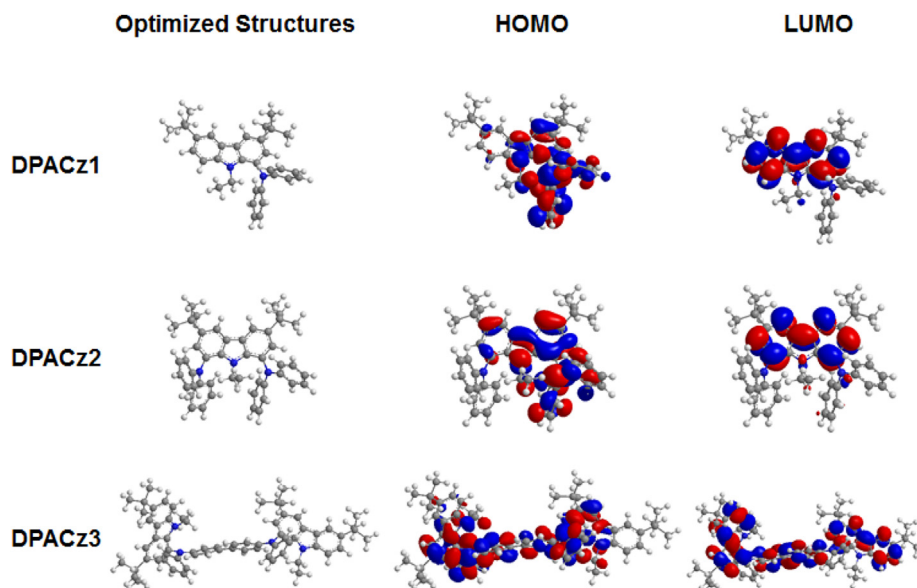


Fig. 3. Optimized Geometrical structures and HOMO & LUMO distributions of **DPACz1**, **DPACz2** and **DPACz3**.

luminous efficiencies of **Device 1** ( $24.5 \text{ cd A}^{-1}$ ) and **Device 2** ( $25.0 \text{ cd A}^{-1}$ ) are similar, while that of **Device 3** ( $11.2 \text{ cd A}^{-1}$ ) is relatively quite low. If we compare these devices with the reference device (**Device 4**) employing the conventional bipolar host material, **26DCzPPy**, we see that the **Devices 1** and **2** perform again better as compared to the reference device, **Device 4**, though the efficiency roll-off is relatively prominent at higher luminance. The origin of the relatively low luminance and prominent efficiency roll-off can be the unipolar hole-transporting characteristics of our **DPACz** materials. Because they do not contain any electron transporting moiety in the molecules, the charge imbalance within the emissive layer can become more and more serious as current

density and luminance increases, which results in passage of current without efficient exciton formation in the emissive layer.

Another point we can find out from the results of these three series of materials, **DPACz1–DPACz3**, is the relative importance of HOMO energy level and triplet energy level of the host materials. As can be easily seen, the luminous efficiency of **Device 3** was the lowest while it had an advantage of the driving voltage. While the HOMO energy levels influence the driving voltage, the triplet energy levels influence the overall device efficiency. This is because the dopant triplet excitons produced during device operation can be transferred back to host in case of the lower triplet energy level of the host than the dopant, which results into non-emissive exciton quenching within the host. Considering the  $E_T$  of **DPACz3** ( $2.45 \text{ eV}$ ) that is still higher than that of  $\text{Ir}(\text{mppy})_3$  ( $\sim 2.4 \text{ eV}$ ) this result gives an experimental guideline of  $E_T$  of host materials, i.e., in order to achieve good performances host should possess  $E_T$  of at least  $0.2 \text{ eV}$  higher than that of the dopant.

Along with the luminous efficiencies, Fig. 5c shows the power efficiency–voltage curves of the four devices. Because the power efficiency of an OLED is closely related to the applied voltage, and our **DPACz** series showed gradual change of operating voltages when applied to OLED devices, the resultant trend among the materials is different from the previous luminous efficiency trend. The maximum power efficiency was obviously the highest for **Device 2** ( $17.9 \text{ lm W}^{-1}$ ), although the luminous efficiency was similar between **Device 1** and **Device 2**. And even **Device 3** also showed comparable power efficiency value,  $10.1 \text{ lm W}^{-1}$ , with the reference device (**Device 4**),  $10.9 \text{ lm W}^{-1}$ . Therefore **DPACz2** which contains two diphenylamino substituents at 1- and 8-position of carbazole has shown the potential of itself as a good solution-processable host material, considering the results presented so far.

In addition to the aforementioned four OLED devices, we further fabricated and investigated three more devices **Device 11**, **Device 22** and **Device 33** in which the emitting layers consisted of 83 wt% of our new host materials, **DPACz1**, **DPACz2** and **DPACz3**, respectively, 10 wt% of a common electron-transporting material 2-(4-biphenyl)-5-(4-*tert*-butylphenyl)-1,3,4-oxadiazole (**PBD**) to adjust the charge balance, and 7 wt% of the emitting dopant,  $\text{Ir}(\text{mppy})_3$ . All the other fabrication process is the same as the previous experiment. The OLED device characteristics are shown in Fig. 6 and

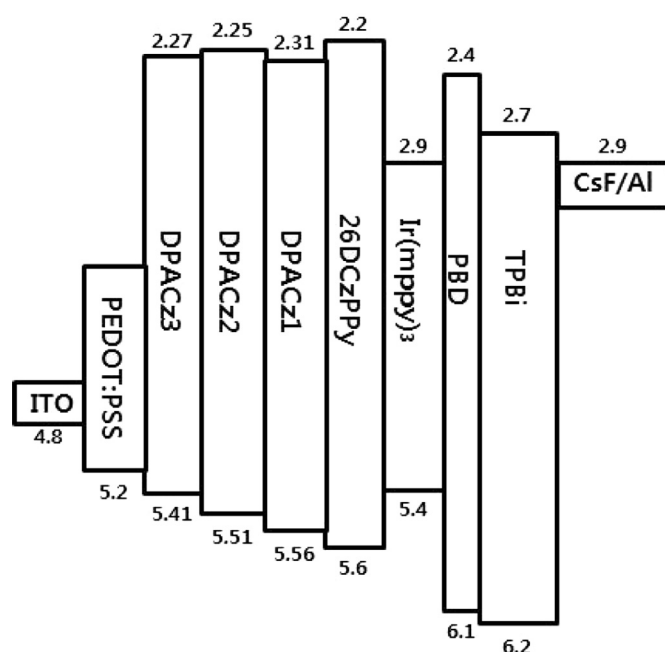


Fig. 4. Energy level diagram of the devices.

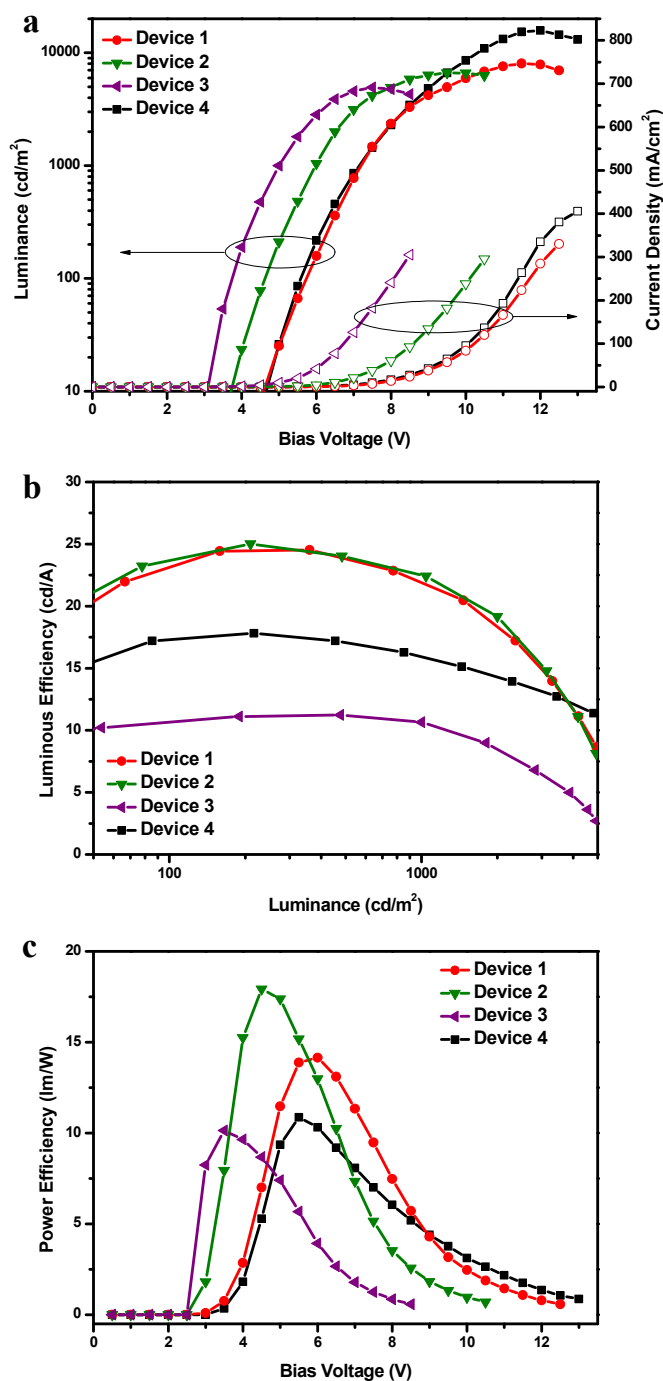


Fig. 5. Device characteristics of Devices 1–4. (a) J–V–L characteristics, (b) luminous efficiency – luminance characteristics, (c) power efficiency – voltage characteristics.

summarized in Table 3. The plotted range of horizontal and vertical axes of each of the graphs in both Figs. 5 and 6 are intentionally set as the same to ease comparison.

The first thing we can easily notice about those PBD-containing mixed host devices is the reduction of the driving voltage (Fig. 6a). In particular, the operating voltage at 1000 cd m<sup>-2</sup> is reduced from 7.2 (Device 1) to 6.0 (Device 11), from 6.0 (Device 2) to 5.6 (Device 22) and from 5.0 (Device 3) to 4.9 V (Device 33). All of these values being less than the reference device (Device 44) using the conventional bipolar host material, 26DCzPPy that operated at 7.1 V. The degree of reduction of the operating voltage increases from

DPACz3 to DPACz1. As the hole-injection barrier increases from Device 3 to Device 1, the charge imbalance of the device can consequently become more and more serious, and this causes an increase of the operating voltage. So, if PBD is added into the emitting layer, the charge imbalance problem could be overcome to a large extent, and this positive effect of PBD is the most prominent in case of the Device 1 where the injection barrier is the largest. The maximum achieved luminance for these PBD-containing mixed host devices were also improved too much as compared to the simple devices, the values being 18,550 (Device 11), 15,530 (Device 22) and 9090 cd m<sup>-2</sup> (Device 33), respectively. It is noteworthy here that incorporation of the PBD as electron transporting moiety in the emitting layer resulted into increasing the luminance by 130% (Device 11), 134% (Device 22) and 84% (Device 33) the values for devices without PBD (Devices 1–3), more possibly because of the more balanced charge transport within the emissive layer.

Along with the operating voltage and the luminance, the improvement of the device efficiencies and the lowering of efficiency roll-off are also distinct (Fig. 6b and c). All of the three devices showed increased luminous efficiencies after PBD addition. The maximum luminous efficiencies of each of the devices were 26.7 cd A<sup>-1</sup> (Device 11), 25.3 cd A<sup>-1</sup> (Device 22) and 14.2 cd A<sup>-1</sup> (Device 33), respectively, while the corresponding values for the reference device (Device 4) were 17.8 cd A<sup>-1</sup>. But what is more important about the luminous efficiencies is the lowering of the efficiency roll-off for all the three devices. Comparison between Figs. 5b and 6b clearly shows that the luminance point where the maximum efficiency was achieved shifted to the higher luminance as a result of PBD addition. In other words, the efficiencies dropped off rapidly under DPACz-host-only conditions (Device 1 to Device 3), because the injected charges could not be utilized efficiently to produce excitons, especially at high luminance with high current density. But in case of improved charge balance with PBD (Device 11 to Device 33), the excitons could be produced more efficiently at high luminance, and the efficiencies could be maintained well [48].

Moreover, the power efficiency results of PBD addition are also interesting. In the case of DPACz host only devices, the Device 2 containing DPACz2 showed the dominant result, but the power efficiency of Device 11 containing DPACz1 could almost reach that of Device 22 after PBD addition. As has been stated in the previous paragraph, the degree of reduction of the operating voltage is the highest in case of DPACz1, therefore a gain in power efficiency can be more than that of DPACz2, which results in similar level of power efficiencies between them.

Electroluminescent (EL) spectra of all of the devices are shown in Fig. 7. As shown in the figure, all devices emit typical green light. The devices incorporating only the new host materials (Devices 1–3) show an additional very weak band in the EL spectra near 407 nm that shows a little incomplete transfer of excitons from hosts to the phosphorescent guest. This, most probably, is due to charge imbalance [49] as in the case of the devices incorporating additional PBD, this band was almost overcome. Another important feature of the EL spectra is the narrowing of the spectrum of the devices containing the new host materials as compared to the 26DCzPPy device. This is an advantageous phenomenon with respect to the colour purity and will be further investigated.

### 3. Experimental

#### 3.1. Materials

Carbazole, tetrabutylammonium bromide (TBAB), bromoethane, anhydrous zinc chloride (ZnCl<sub>2</sub>), *N*-bromosuccinimide (NBS), diphenylamine, sodium *tert*-butoxide (<sup>t</sup>BuONa), and tris(dibenzylideneacetone) dipalladium (0) [Pd<sub>2</sub>(dba)<sub>3</sub>] were purchased from

**Table 3**  
Electroluminescence data of the Devices 1–4 and 11–33.

Devices	V <sub>on</sub> [V] (10 nit)	V [V] (1000 nit)	η <sub>c</sub> [cd A <sup>-1</sup> ] (1000 nit)	η <sub>p</sub> [lm W <sup>-1</sup> ] (1000 nit)	η <sub>ext</sub> [%] (1000 nit)	η <sub>c,max</sub> [cd A <sup>-1</sup> ]	η <sub>p,max</sub> [lm W <sup>-1</sup> ]	η <sub>ext,max</sub> [%]	L <sub>max</sub> [cd m <sup>-2</sup> ]	CIE coordinates
Device 1	4.6	7.2	22.1	10.7	7.2	24.5	14.1	8.0	8,050	(0.290, 0.602)
Device 2	3.7	6.0	22.5	13.1	7.3	25.0	17.9	8.2	6,632	(0.289, 0.606)
Device 3	3.1	5.0	10.7	7.4	3.5	11.2	10.1	3.6	4,936	(0.293, 0.605)
Device 4	4.6	7.1	15.9	7.8	5.0	17.8	10.9	5.6	15,720	(0.318, 0.611)
Device 11	4.3	6.0	26.6	15.4	8.5	26.7	16.5	8.5	18,550	(0.297, 0.609)
Device 22	4.0	5.6	24.9	15.5	8.0	25.3	16.9	8.1	15,530	(0.295, 0.607)
Device 33	3.1	4.9	13.4	9.6	4.3	14.2	12.5	4.6	9,090	(0.296, 0.608)

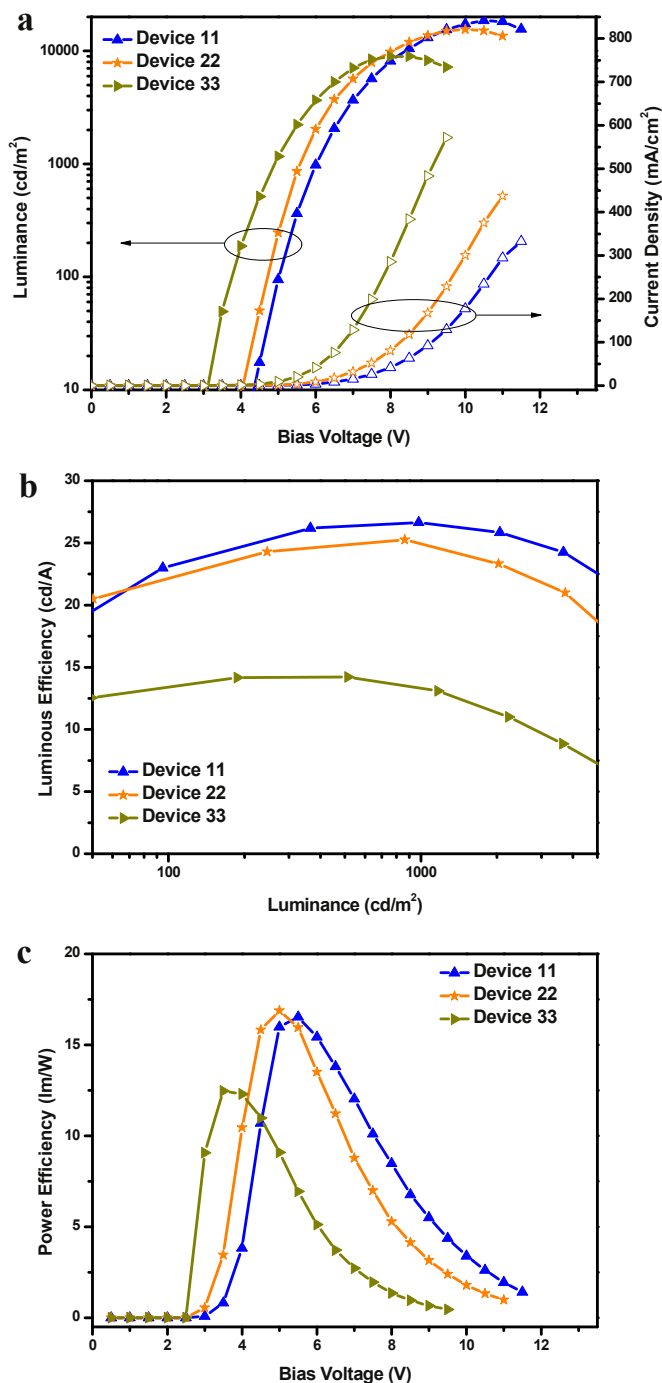


**Fig. 6.** Device characteristics of Devices 11–33. (a) J–V–L characteristics, (b) luminous efficiency – luminance characteristics, (c) power efficiency – voltage characteristics.

Sigma–Aldrich Co. *tert*-Butylchloride (<sup>t</sup>BuCl) was purchased from Wako Pure Chemical Industries Ltd. N<sup>4</sup>,N<sup>4'</sup>-diphenylbenzidine was purchased from TCI Co., Ltd. and tri-*tert*-butylphosphine (P(<sup>t</sup>Bu)<sub>3</sub>) was purchased from Kanto Chemical Co., Inc. All the reagents were used as received without further purification.

### 3.2. Instrumentation

<sup>1</sup>H and <sup>13</sup>C NMR spectra were measured using Bruker DPX-300 NMR spectrometers. Differential scanning calorimetry (DSC) was conducted using a DSC Q1000 TA Instrument Inc. (V9.9 Build 303). UV–vis. absorption spectra were obtained using SHIMADZU UV-2550 spectrophotometer and room temperature & low temperature photoluminescence spectra were obtained using Perkin Elmer LS55 luminescence spectrometer. Atomic force microscopy (AFM) measurements were conducted on Bruker MultiMode8 by tapping mode. Cyclic voltammetry was performed with BAS 100B electrochemical analyzer. The electrical characteristics of the devices were characterized by Keithley 2400 source measurement unit. The luminance and emission spectrum of OLED devices were characterized by Konica-Minolta CS-100A luminance meter and CS-1000 spectroradiometer, respectively. All measurements of the fabricated devices were carried out at room temperature under ambient conditions.

### 3.3. Syntheses

#### 3.3.1. Synthesis of 3,6-di-*tert*-butyl-9H-carbazole (1)

Carbazole (16.7 g, 100 mmol), 200 mL of nitromethane, and ZnCl<sub>2</sub> (40.5 g, 300 mmol) were added to a two-neck flask under a nitrogen atmosphere. 2-Chloro-2-methylpropane (32.5 mL,

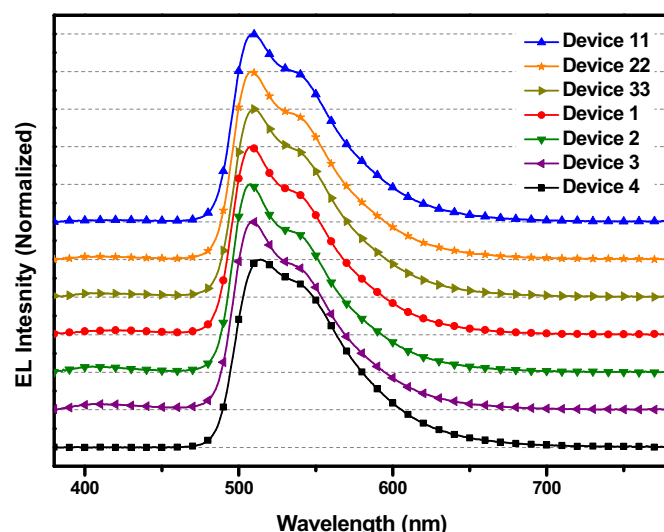


**Fig. 7.** EL spectra of Devices 1–4 and 11–33.

300 mmol) was added drop-wise under stirring. The mixture was stirred at room temperature for 5 h followed by hydrolysis with 500 mL of water. The product was extracted with CH<sub>2</sub>Cl<sub>2</sub> (3 × 200 mL). The organic layer was washed with H<sub>2</sub>O (2 × 300 mL), dried over MgSO<sub>4</sub>, and evaporated under vacuum to yield 25.4 g (91%) of a light green solid which was recrystallized from absolute ethanol to get an off-white solid.

<sup>1</sup>H NMR (300 MHz, CDCl<sub>3</sub>, ppm): δ = 8.07 (s, 2H), 7.85 (s, 1H), 7.47 (m, 2H), 7.33 (d, *J* = 8.4 Hz, 2H), 1.45 (s, 18H).

<sup>13</sup>C NMR (100 MHz, CDCl<sub>3</sub>, ppm): δ = 142.20, 138.00, 123.49, 123.29, 116.15, 109.98, 34.68, 32.03.

### 3.3.2. Synthesis of 1-bromo-3,6-di-*tert*-butyl-9H-carbazole (2)

To a solution of (1) (10.5 g, 37.5 mmol) in DMF (100 mL), a solution of *N*-bromosuccinimide (6.66 g, 37.5 mmol) in DMF (10 mL) was added drop-wise, under light protection, over 10 min, and the mixture was stirred at room temperature for 3 h. Water (300 mL) was added and the resulting mixture was extracted with CH<sub>2</sub>Cl<sub>2</sub> (50 mL × 3). The combined organic phase was washed with water (150 mL × 2), dried over anhydrous MgSO<sub>4</sub>, and evaporated in vacuo where upon an off white sticky liquid was obtained which was subjected to silica gel column chromatography (hexane/dichloromethane, 4/1) to get a colourless oil. This oil was dissolved in methanol followed by evaporation of the solvent to get a white glassy solid (11.5 g, 85.4%).

<sup>1</sup>H NMR (300 MHz, CDCl<sub>3</sub>, ppm): 8.05 (m, 3H), 7.59 (d, *J* = 1.5 Hz, 1H), 7.52 (m, 1H), 7.39 (m, 1H), 1.45 (s, 9H), 1.44 (s, 9H).

<sup>13</sup>C NMR (100 MHz, CDCl<sub>3</sub>, ppm): δ = 144.00, 142.89, 137.73, 136.69, 125.72, 124.61, 124.34, 123.62, 116.62, 115.45, 110.51, 103.66, 34.86, 34.73, 31.97, 30.90.

### 3.3.3. Synthesis of 3,6-di-*tert*-butyl-9-ethyl-9H-carbazole (3)

To a stirred solution of 3,6-di-*tert*-butyl-9H-carbazole (5.59 g, 20 mmol) and tetrabutylammonium bromide (TBAB) (0.32 g, 1 mmol) in acetone (30 mL) was added, drop-wise, bromoethane (3.0 g, 27.5 mmol). After stirring for 5 min, powdered NaOH (1.1 g, 27.5 mmol) was added in three portions and the reaction mixture was heated under reflux until the reaction was complete (1 h). Water (100 mL) was added and the product was extracted with ethyl acetate (50 mL). The organic layer was separated, washed with water, dried over MgSO<sub>4</sub> and concentrated. Pure product (5.7 g, 92.7%) was obtained as white solid was obtained upon recrystallization from ethanol.

<sup>1</sup>H NMR (300 MHz, CDCl<sub>3</sub>, ppm): δ = 8.10 (d, *J* = 1.5 Hz, 2H), 7.51 (dd, *J* = 6.9, 1.8 Hz, 2H), 7.32 (d, *J* = 8.7 Hz, 2H), 4.35 (q, *J* = 6.9 Hz, 2H), 1.46 (s, 18H), 1.44 (t, *J* = 7.2 Hz, 3H).

<sup>13</sup>C NMR (100 MHz, CDCl<sub>3</sub>, ppm): δ = 141.47, 138.49, 123.24, 122.79, 116.37, 107.81, 37.55, 34.69, 32.11, 13.99.

### 3.3.4. Synthesis of 1-bromo-3,6-di-*tert*-butyl-9-ethyl-9H-carbazole (4)

Compound (4) was prepared using the same procedure as for (3) using (2) (7.17 g, 20 mmol), the other reagents being in the same amounts as in case of (3). Pure product 7.1 g (92.2%) as a white crystalline solid was obtained by recrystallization from absolute ethanol. <sup>1</sup>H NMR (300 MHz, CDCl<sub>3</sub>, ppm): δ = 8.05 (d, *J* = 1.5 Hz, 1H), 8.02 (d, *J* = 1.5 Hz, 1H), 7.60 (d, *J* = 1.8 Hz, 1H), 7.55 (dd, *J* = 1.8, 8.7 Hz, 1H), 7.34 (d, *J* = 8.7 Hz, 1H), 4.75 (q, *J* = 7.2 Hz, 2H), 1.45 (s, 9H), 1.43 (s, 9H), 1.42 (t, *J* = 7.2 Hz, 3H).

<sup>13</sup>C NMR (100 MHz, CDCl<sub>3</sub>, ppm): δ = 143.19, 142.47, 139.60, 135.00, 128.66, 126.25, 124.22, 122.31, 116.07, 115.52, 108.46, 102.33, 38.78, 34.70, 34.56, 32.00, 31.87, 15.61.

### 3.3.5. Synthesis of 1,8-dibromo-3,6-di-*tert*-butyl-9-ethyl-9H-carbazole (5)

Compound (5) was prepared following the method used for the preparation of (2) using (3) (3.07 g, 10 mmol), DMF (30 mL), and NBS (3.56 g, 20 mmol). Pure product (4.1 g, 88.4%) was obtained as white crystals upon recrystallization from absolute ethanol.

<sup>1</sup>H NMR (300 MHz, CDCl<sub>3</sub>, ppm): δ = 7.96 (d, *J* = 1.5 Hz, 1H), 7.65 (d, *J* = 1.8 Hz, 1H), 5.22 (q, *J* = 7.2 Hz, 2H), 1.43 (s, 18H), 1.39 (t, *J* = 6.9 Hz, 3H).

<sup>13</sup>C NMR (100 MHz, CDCl<sub>3</sub>, ppm): δ = 144.16, 136.09, 130.27, 126.20, 115.30, 103.04, 39.30, 34.57, 31.77, 17.12.

### 3.3.6. General procedure for Buchwald–Hartwig coupling

A mixture of the bromocompound (1 mol. eq. w.r.t. Br), diarylamine (1 mol. eq. w.r.t. NH), Pd<sub>2</sub>(dba)<sub>3</sub> (5 mol.% eq.), <sup>t</sup>Bu<sub>3</sub>P (20 mol.%), and <sup>t</sup>BuONa (3 mol. eq.) in toluene was heated under N<sub>2</sub> atmosphere at reflux temperature for 10–20 h. The reaction mixture was then filtered. The filtrate was evaporated under vacuum and the residue was subjected to column chromatography on silica gel.

### 3.3.7. Synthesis of 3,6-di-*tert*-butyl-9-ethyl-*N,N*-diphenyl-9H-carbazol-1-amine (DPACz1)

Compound (5) was prepared by employing the general Pd-catalyzed coupling procedure using (3) (0.966 g, 2.5 mmol), diphenylenediamine (0.457 g, 2.7 mmol), Pd<sub>2</sub>(dba)<sub>3</sub> (0.116 g, 0.127 mmol), <sup>t</sup>Bu<sub>3</sub>P (0.104 g, 0.507 mmol), and <sup>t</sup>BuONa (0.72 g, 7.5 mmol) in toluene (10 mL). (5) was obtained as a white solid (0.99 g, 83.9%) by column chromatography (*n*-Hexane/DCM, 2:1).

<sup>1</sup>H NMR (400 MHz, CDCl<sub>3</sub>, ppm): δ = 8.10 (d, *J* = 1.2 Hz, 1H), 8.03 (d, *J* = 2.0 Hz, 1H), 7.50 (dd, *J* = 8.8, 2.0 Hz, 1H), 7.24 (d, *J* = 8.8 Hz, 1H), 7.20–7.16 (m, 5H), 7.08 (d, 8.0 Hz, 4H), 6.90 (t, *J* = 7.2 Hz, 2H), 4.36 (q, *J* = 6.8 Hz, 2H), 1.45 (s, 9H), 1.36 (s, 9H), 0.87 (t, *J* = 6.8 Hz, 3H).

<sup>13</sup>C NMR (75 MHz, CDCl<sub>3</sub>, ppm): δ = 147.72, 143.20, 142.03, 139.10, 135.02, 129.33, 129.01, 126.86, 125.69, 123.64, 122.94, 121.28, 120.97, 115.90, 114.72, 108.67, 39.04, 34.66, 34.54, 32.04, 31.88, 14.39.

HRMS (EI+): calculated for C<sub>34</sub>H<sub>38</sub>N<sub>2</sub>, 474.3035; found, 474.3026.

### 3.3.8. Synthesis of 3,6-di-*tert*-butyl-9-ethyl-*N1,N1,N8,N8*-tetraphenyl-9H-carbazole-1,8-diamine (DPACz2)

Compound (6) was prepared by employing the general Pd-catalyzed coupling procedure using (4) (0.233 g, 0.5 mmol), diphenylenediamine (0.22 g, 1.3 mmol), Pd<sub>2</sub>(dba)<sub>3</sub> (0.046 g, 0.05 mmol), <sup>t</sup>Bu<sub>3</sub>P (0.041 g, 0.20 mmol), and <sup>t</sup>BuONa (0.144 g, 1.5 mmol) in toluene (5 mL). Compound (6) was obtained as a white solid (0.20 g, 62.3%) upon column chromatography (*n*-Hexane/DCM, 2:1).

<sup>1</sup>H NMR (400 MHz, CDCl<sub>3</sub>, ppm): δ = 7.99 (d, *J* = 1.6 Hz, 2H), 7.19 (d, *J* = 2.0 Hz, 2H), 7.12 (d, *J* = 8.4 Hz, 4H), 7.10 (d, *J* = 7.2 Hz, 4H), 6.97 (d, 8.0 Hz, 8H), 6.87 (t, *J* = 7.2 Hz, 4H), 4.26 (q, *J* = 6.8 Hz, 2H), 1.35 (s, 18H), 0.65 (t, *J* = 6.8 Hz, 3H).

<sup>13</sup>C NMR (75 MHz, CDCl<sub>3</sub>, ppm): δ = 147.50, 143.99, 135.83, 130.82, 128.87, 126.91, 126.84, 121.49, 121.22, 113.94, 39.89, 34.56, 31.81, 15.24.

HRMS (EI+): calculated for C<sub>34</sub>H<sub>38</sub>N<sub>2</sub>, 641.3770; found, 641.3766.

### 3.3.9. Synthesis of *N4,N4'*-bis(3,6-di-*tert*-butyl-9-ethyl-9H-carbazol-1-yl)-*N4,N4'*-diphenyl-[1,1'-biphenyl]-4,4'-diamine (DPACz3)

Compound (7) was prepared by employing the general Pd-catalyzed coupling procedure using (3) (0.772 g, 2 mmol), *N4,N4'*-diphenylbenzidine (0.336 g, 1 mmol), Pd<sub>2</sub>(dba)<sub>3</sub> (0.092 g, 0.1 mmol), <sup>t</sup>Bu<sub>3</sub>P (0.081 g, 0.4 mmol), and <sup>t</sup>BuONa (0.577 g,

6.0 mmol) in toluene (10 mL). Pure product was obtained as a white solid (0.66 g, 69.8%) upon column chromatography (*n*-Hexane/DCM, 2:1).

$^1\text{H}$  NMR (400 MHz,  $\text{CDCl}_3$ , ppm):  $\delta$  = 8.10 (d,  $J$  = 1.6 Hz, 2H), 8.04 (d,  $J$  = 1.6 Hz, 2H), 7.50 (dd,  $J$  = 8.4, 1.6 Hz, 2H), 7.39 (d,  $J$  = 8.4 Hz, 4H), 7.25–7.17 (m, 7H), 7.10 (d, 8.8 Hz, 7H), 6.91 (t,  $J$  = 7.2 Hz, 2H), 4.36 (m, 2H), 1.45 (s, 18H), 1.37 (s, 18H), 0.90 (t,  $J$  = 7.2 Hz, 3H).

$^{13}\text{C}$  NMR (100 MHz,  $\text{CDCl}_3$ , ppm):  $\delta$  = 147.58, 146.50, 143.24, 142.06, 139.12, 135.01, 133.42, 129.19, 129.05, 126.91, 126.78, 125.76, 123.68, 122.95, 121.33, 121.16, 120.98, 115.91, 114.81, 108.69, 39.07, 34.65, 34.56, 32.03, 31.89, 14.47.

HRMS (EI<sup>+</sup>): calculated for  $\text{C}_{34}\text{H}_{38}\text{N}_2$ , 946.5913; found, 946.5875.

#### 3.4. Device fabrication and measurements

Commercially available hole-injection material poly-(3,4-ethylenedioxythiophene):poly-(styrenesulfonate) (PEDOT:PSS), hole/exciton-blocking/electron-transporting material 1,3,5-tris(N-phenylbenzimidazol-2-yl)benzene (TPBI) were used. Commercial indium tin oxide (ITO) coated glass with sheet resistance of 10  $\Omega$  per square was used as the starting substrates. The substrates were pre-cleaned carefully and treated by oxygen plasma for 2 min before device fabrication followed by spin-coating PEDOT:PSS (35 nm) which was dried then at 120 °C for 30 min under vacuum. Then the emissive layer (40 nm) of host materials doped with 7 wt% green emitting dopant, Ir(mppy)<sub>3</sub> was spin-coated from chlorobenzene solution onto the PEDOT:PSS layer and dried at 80 °C for 30 min to remove residual solvent followed by thermal deposition of electron transport layer (ETL) of TPBI (57 nm), and a cathode composed of cesium fluoride (CsF, 1 nm) and aluminium (Al, 80 nm) successively at 10<sup>−6</sup> Torr.

#### 4. Conclusions

We report three novel diphenylaminocarbazole materials, **DPACz1**, **DPACz2** and **DPACz3**, making use of the less explored 1- and 8-positions of carbazole. The structures of the final products were confirmed by  $^1\text{H}$  NMR,  $^{13}\text{C}$  NMR and HRMS measurements. The compounds have high triplet energy levels as determined from the phosphorescence spectra at low temperature. High triplet energies along with shallow HOMO levels suggested the use of the materials as suitable host materials for green PhOLEDs. Solution processed bilayer devices with configuration, [ITO/PEDOT:PSS/Emitting layer/TPBi/CsF/Al], fabricated by using the new materials as hosts show high luminous and power efficiencies as well as low turn-on voltages. All devices emitted typical green light with high luminance and have low turn-on voltages. Improvement in the efficiencies and suppression of efficiency roll-off was further achieved by using the common electron transporting material PBD as a co-host in the emissive layer.

#### Acknowledgements

This work was supported by the Global Leading Technology Program funded by the Ministry of Trade, Industry and Energy, Republic of Korea (Project No. 10042477) and by the R&D Convergence Program of NST (National Research Council of Science & Technology) of Republic of Korea (Younghapsilyonghwa-13-10-KITECH).

#### Appendix A. Supplementary data

Supplementary data related to this article can be found at <http://dx.doi.org/10.1016/j.dyepig.2015.08.027>.

#### References

- [1] Weiss DS, Abkowitz M. Advances in organic photoconductor technology. *Chem Rev* 2010;39:479–86.
- [2] Hains AW, Liang Z, Woodhouse MA, Gregg BA. Molecular semiconductors in organic photovoltaic cells. *Chem Rev* 2010;39:6689–735.
- [3] Yook KS, Lee JY. Small molecule host materials for solution processed phosphorescent organic light-emitting diodes. *Adv Mater* 2014;26:4218–33.
- [4] Baldo MA, O'Brien DF, You Y, Shoustikov A, Sibley S, Thompson ME, et al. Highly efficient phosphorescent emission from organic electroluminescent devices. *Nature* 1998;395:151–4.
- [5] Zhao Z, Xu X, Wang H, Lu P, Yu G, Liu Y. Zigzag molecules from pyrene-modified carbazole oligomers: synthesis, characterization, and application in OLEDs. *J Org Chem* 2008;73:594–602.
- [6] Tria MC, Liao K-S, Alley N, Curran S, Advincula R. Electrochemically cross-linked surface-grafted PVK polymer brushes as a hole transport layer for organic photovoltaics. *J Mater Chem* 2011;21:10261–4.
- [7] Park JJ, Park TJ, Jeon WS, Pode R, Jang J, Kwon JH, et al. Small molecule interlayer for solution processed phosphorescent organic light emitting device. *Org Electron* 2009;10:189–93.
- [8] Nomura M, Shibasaki Y, Ueda M, Tugita K, Ichikawa M, Taniguchi Y. Synthesis of thermally stable and hole-transporting amorphous molecule having four carbazole moieties. *Synth Met* 2005;148:155–60.
- [9] Wong WY, Ho CL. Functional metallophosphors for effective charge carrier injection/transport: new robust OLED materials with emerging applications. *J Mater Chem* 2009;19:4457–82.
- [10] Kim SH, Cho I, Sim MK, Park S, Park SY. Highly efficient deep-blue emitting organic light emitting diode based on the multifunctional fluorescent molecule comprising covalently bonded carbazole and anthracene moieties. *J Mater Chem* 2011;21:9139–48.
- [11] Nishimoto T, Yasuda T, Lee SY, Kondo R, Adachi C. A six-carbazole-decorated cyclophosphazene as a host with high triplet energy to realize efficient delayed-fluorescence OLEDs. *Mater Horiz* 2014;1:264–9.
- [12] Brunner K, van Dijken A, Börner H, Bastiaansen JJAM, Kiggen NMM, Langeveld BMW. Carbazole compounds as host materials for triplet emitters in organic light-emitting diodes: tuning the HOMO level without influencing the triplet energy in small molecules. *J Am Chem Soc* 2004;126:6035–42.
- [13] Sasabe H, Toyota N, Nakanishi H, Ishizaka T, Pu YJ, Kido J. 3,3'-Bicarbazole-based host materials for high-efficiency blue phosphorescent OLEDs with extremely low driving voltage. *Adv Mater* 2012;24:3212–7.
- [14] Zaleckas E, Griniene R, Stulpinaite B, Grazulevicius JV, Liu L, Xie Z, et al. Electroactive polymers containing pendant harmaline, phenoxazine or carbazole rings as host materials for OLEDs. *Dyes Pigments* 2014;108:121–5.
- [15] Schrogel P, Tomkeviciene A, Stroehriegel P, Hoffmann ST, Kohlerb A, Lennartz C. A series of CBP-derivatives as host materials for blue phosphorescent organic light-emitting diodes. *J Mater Chem* 2011;21:2266–73.
- [16] Cui L-S, Dong S-C, Liu Y, Li Q, Jiang Z-Q, Liao L-S. A simple systematic design of phenylcarbazole derivatives for host materials to high-efficiency phosphorescent organic light-emitting diodes. *J Mater Chem C* 2013;1:3967–75.
- [17] Hu D, Lu P, Wang C, Liu H, Wang H, Wang Z, et al. Silane coupling dicarbazoles with high triplet energy as host materials for highly efficient blue phosphorescent devices. *J Mater Chem* 2009;19:6143–8.
- [18] Shirota Y, Kageyama H. Charge carrier transporting molecular materials and their applications in devices. *Chem Rev* 2007;107:953–1010.
- [19] Fu Q, Chen J, Shi C, Ma D. Solution-processed small molecules as mixed host for highly efficient blue and white phosphorescent organic light-emitting diodes. *ACS Appl Mater Interfaces* 2012;4:6579–86.
- [20] Fan C, Chen Y, Jiang Z, Yang C, Zhong C, Qin J, et al. Diarylmethylene-bridged triphenylamine derivatives encapsulated with fluorene: very high T<sub>g</sub> host materials for efficient blue and green phosphorescent OLEDs. *J Mater Chem* 2010;20:3232–7.
- [21] Jiang W, Duan L, Qiao J, Dong G, Zhang D, Wang L, et al. High-triplet-energy tri-carbazole derivatives as host materials for efficient solution-processed blue phosphorescent devices. *J Mater Chem* 2011;21:4918–26.
- [22] Deng L, Li J, Li W. Solution-processible small-molecular host materials for high-performance phosphorescent organic light-emitting diodes. *Dyes Pigments* 2014;102:150–8.
- [23] Lin M-S, Chi L-C, Chang H-W, Huang Y-H, Tien K-C, Chen C-C, et al. A diarylborane-substituted carbazole as a universal bipolar host material for highly efficient electrophosphorescence devices. *J Mater Chem* 2012;22:870–6.
- [24] Krucaite G, Tavgeniene D, Grazulevicius JV, Wang YC, Hsieh CY, Jou JH, et al. 3,6-Diaryl substituted 9-alkylcarbazoles as hole transporting materials for various organic light emitting devices. *Dyes Pigments* 2014;106:1–6.
- [25] Gibson VC, Spitzmesser SK, White AJP, Williams DJ. Synthesis and reactivity of 1,8-bis(imino)carbazolide complexes of iron, cobalt and manganese. *Dalton Trans* 2003:2718–27.
- [26] Chu J-H, Wu C-C, Chang D-H, Lee Y-M, Wu M-J. Direct ortho arylation of 9-(pyridin-2-yl)-9H-carbazoles bearing a removable directing group via palladium(II)-catalyzed C–H bond activation. *Organometallics* 2013;32:272–82.
- [27] Hao Q, Yu S, Li S, Chen J, Zeng Y, Yu T, et al. Locked planarity: a strategy for tailoring ladder-type  $\pi$ -conjugated anilido-pyridine boron difluorides. *J Org Chem* 2014;79:459–64.

- [28] Inoue M, Suzuki T, Nakada M. Asymmetric catalysis of Nozaki–Hiyama allylation and methallylation with a new tridentate bis(oxazolonyl)carbazole ligand. *J Am Chem Soc* 2003;125:1140–1.
- [29] Huang H, Fu Q, Pan B, Zhuang S, Wang L, Chen J, et al. Butterfly-shaped tetrasubstituted carbazole derivatives as a new class of hosts for highly efficient solution-processable green phosphorescent organic light-emitting diodes. *Org Lett* 2012;14:4786–9.
- [30] Gong W-L, Zhong F, Aldred MP, Fu Q, Chen T, Huang D-K, et al. Carbazole oligomers revisited: new additions at the carbazole 1- and 8-positions. *RSC Adv* 2012;2:10821–8.
- [31] Wang H-Y, Liu F, Xie L-H, Tang C, Peng B, Huang W, et al. Topological arrangement of fluorenyl-substituted carbazole triads and starbursts: synthesis and optoelectronic properties. *J Phys Chem C* 2011;115:6961–7.
- [32] Kochapradist P, Prachumrak N, Tarsang R, Keawin T, Jungsuttiwong S, Sudyoasuk T, et al. Multi-triphenylamine-substituted carbazoles: synthesis, characterization, properties, and applications as hole-transporting materials. *Tetrahedron Lett* 2013;54:3683–7.
- [33] Kato S-I, Noguchi H, Kobayashi A, Yoshihara T, Tobita S, Nakamura Y. Bicarbazoles: systematic structure–property investigations on a series of conjugated carbazole dimers. *J Org Chem* 2012;77:9120–33.
- [34] Tomkeviciene A, Puckyte G, Grazulevicius JV, Degbia M, Tran-Van F, Schmaltz B, et al. Diphenylamino-substituted derivatives of 9-phenylcarbazole as glass-forming hole-transporting materials for solid state dye sensitized solar cells. *Synth Met* 2012;162:1997–2004.
- [35] Sakalyte A, Simokaitiene J, Tomkeviciene A, Keruckas J, Buika G, Grazulevicius JV, et al. Effect of methoxy substituents on the properties of the derivatives of carbazole and diphenylamine. *J Phys Chem C* 2011;115:4856–62.
- [36] Sun J, Jiang H-J, Zhang J-L, Tao Y, Chen R-F. Synthesis and characterization of heteroatom substituted carbazole derivatives: potential host materials for phosphorescent organic light-emitting diodes. *New J Chem* 2013;37:977–85.
- [37] Grigalevicius S, Buika G, Grazulevicius JV, Gaidelis V, Jankauskas V, Montrimas E. 3,6-Di(diphenylamino)-9-alkylcarbazoles: novel hole-transporting molecular glasses. *Synth Met* 2001;311–4.
- [38] Tomkeviciene A, Puckyte G, Grazulevicius JV, Kazlauskas K, Jursenas S, Jankauskas V. Dimethyldiphenylamino-substituted carbazoles as electronically active molecular materials. *Dyes Pigments* 2013;96:574–80.
- [39] Lia L-J, Bai F-Q, Zhang H-X. Theoretical studies of the structural, electronic and optical properties of carbazole-based compounds. *J Phys Org Chem* 2012;25:334–42.
- [40] Liu Y, Nishiura M, Wang Y, Hou Z.  $\pi$ -Conjugated aromatic enynes as a single-emitting component for white electroluminescence. *J Am Chem Soc* 2006;128:5592–3.
- [41] Araneda JF, Piers WE, Heyne B, Parvez M, McDonald R. High stokes shift anilido-pyridine boron difluoride dyes. *Angew Chem Int Ed* 2011;50:12214–7.
- [42] Ostrauskaite J, Strohriegel P. Formation of macrocycles in the synthesis of poly(N-(2-ethylhexyl)carbazol-3,6-diyl). *Macromol Chem Phys* 2003;204:1713–8.
- [43] Li Z, Wu Z, Fu W, Wang D, Liu P, Jiao B, et al. Stable amorphous bis(dialkylamino)biphenyl derivatives as hole-transporting materials in OLEDs. *Electron Mater Lett* 2013;9:655–61.
- [44] Li G, Zhou Y-F, Cao X-B, Bao P, Jiang K-J, Lin Y, et al. Novel TPD-based organic D- $\pi$ -A dyes for dye-sensitized solar cells. *Chem Commun* 2009:2201–3.
- [45] Yamashita K, Mori T, Mizutani T, Miyazaki H, Takeda T. EL properties of organic light-emitting-diode using TPD derivatives with diphenylstylyl groups as hole transport layer. *Thin Solid Films* 2000;363:33–6.
- [46] Mondal E, Hung W-Y, Dai H-C, Chen H-F, Hung P-Y, Wong K-T. New universal bipolar host materials with fluorene as non-conjugated bridge for multi-color electrophosphorescent devices. *Tetrahedron* 2014;70:6328–36.
- [47] Lee J, Han H, Lee J, Yoon SC, Lee C. Utilization of “thiol-ene” photo cross-linkable hole-transporting polymers for solution-processed multilayer organic light-emitting diodes. *J Mater Chem C* 2014;2:1474–81.
- [48] Lee J, Lee JI, Lee JY, Chu HY. Stable efficiency roll-off in blue phosphorescent organic light-emitting diodes by host layer engineering. *Org Electron* 2009;10:1529–33.
- [49] Lee J, Lee JI, Lee JW, Chu HY. Effects of charge balance on device performances in deep blue phosphorescent organic light-emitting diodes. *Org Electron* 2010;11:1159–64.